

## 1 PlanetScope data

The following tables list scene IDs and acquisition parameters of all PlanetScope data used in this study.

**Table S1.** List of PlanetScope L3B scenes and corresponding metadata across the Sigvas landslide acquired within an approx. 1.5 month period. All scenes were correlated with each other to determine which acquisition parameters determine the strength of the orthorectification error seen in the disparity maps. The quality column indicates whether images have passed all image quality metrics in the processing pipeline. The use of quality category "standard" is recommended. We included a few "test" images, particularly for the identification of the orthorectification error signal at the Sigvas site, to keep a short temporal baseline.

Scene ID	Date of Acquisition	View Angle	Satellite Azimuth	Quality
20220707_144112_41_247c	2022-07-07	4.1	278.3	standard
20220712_142347_87_2262	2022-07-12	5	278.6	standard
20220713_141250_01_2212	2022-07-13	0.1	353.3	standard
20220716_144128_52_2478	2022-07-16	5	278.8	standard
20220717_143827_66_2470	2022-07-17	4	96.5	standard
20220723_143904_82_2478	2022-07-23	0.1	359.4	standard
20220724_140731_82_245c	2022-07-24	1.1	283	standard
20220731_145317_96_2414	2022-07-31	3	94.3	test
20220801_143753_11_2490	2022-08-01	5	96.8	test
20220802_143920_28_2480	2022-08-02	1	281.4	test
20220803_144118_87_2482	2022-08-03	5	278.8	test
20220804_140158_24_2460	2022-08-04	5	96.8	standard
20220806_145017_17_2424	2022-08-06	0.6	8.3	test
20220809_145704_40_2426	2022-08-09	4	279	test
20220812_140836_60_241f	2022-08-12	4	279.2	standard
20220814_143747_50_248b	2022-08-14	4	96.2	standard
20220823_145618_97_2407	2022-08-23	0.1	348.9	standard

**Table S2.** List of PlanetScope L3B scenes and corresponding metadata used for offset tracking across the Siguas landslide separated by processing groups.

<b>Group</b>	<b>Scene ID</b>	<b>Date of Acquisition</b>	<b>View Angle</b>	<b>Satellite Azimuth</b>	<b>Quality</b>
1	20200717_141850_23_2278	2020-07-17	3.9	279.4	standard
	20210302_142459_17_2231	2021-03-02	4	278.4	standard
	20210901_141429_62_242b	2021-09-01	4.1	279.3	standard
	20220108_141431_75_2212	2022-01-08	4	279.4	standard
	20220220_144136_13_2490	2022-02-20	4	279.3	standard
	20220707_144112_41_247c	2022-07-07	4.1	278.3	standard
	20221221_140616_42_2430	2022-12-21	4.5	278.6	standard
2	20201122_150654_13_2416	2020-11-22	3	96.2	test
	20210111_150637_23_2406	2021-01-11	3	96.3	standard
	20210406_142246_83_2231	2021-04-06	3	97.9	standard
	20211002_141111_60_2428	2021-10-02	3.1	95.9	standard
	20211208_141111_53_2465	2021-12-08	3	96.3	standard
	20220413_140614_39_2455	2022-04-13	3	95.9	standard
	20220629_142321_02_2251	2022-06-29	3	95.7	standard
	20221215_145536_42_2413	2022-12-15	3.3	96	standard
20230228_144044_35_2489	2023-02-28	3.1	94.4	standard	
3	20200329_141432_68_2271	2020-03-29	0.1	2	standard
	20200926_150927_49_241c	2020-09-26	0.1	355.1	test
	20201113_142248_59_2441	2020-11-13	0.2	3.3	standard
	20210307_150627_51_2401	2021-03-07	0.2	348.7	standard
	20210514_141500_24_2458	2021-05-14	0.1	359.1	standard
	20210702_141333_57_2460	2021-07-02	0.2	345.7	standard
	20210921_141221_26_2464	2021-09-21	0.3	4	standard
	20220616_143858_18_2488	2022-06-16	0.1	2.6	standard
	20221020_143849_06_2488	2022-10-20	0.4	14.8	standard
4	20200926_150927_49_241c	2020-09-26	0.1	355.1	test
	20210309_142212_90_222f	2021-03-09	5	96.5	standard
	20210705_141517_63_241a	2021-07-05	5	279	standard
	20220506_140845_16_2439	2022-05-06	1	91.9	standard
	20221002_143906_84_2495	2022-10-02	2	95.2	standard
	20221206_143747_18_2488	2022-12-06	4.9	96.6	standard
	20230106_140514_50_2429	2023-01-06	1.2	281.3	standard
20230305_144147_03_24a5	2023-03-05	3.8	279.1	standard	

**Table S3.** List of PlanetScope L3B scenes and corresponding metadata used for offset tracking across the Del Medio landslide separated by processing groups.

Group	Scene ID	Date of Acquisition	View Angle	Satellite Azimuth	Quality
1	20200516_134707_21_2277	2020-05-16	5	279.8	standard
	20200729_134905_10_2277	2020-07-29	5	279.6	standard
	20200905_134846_16_222b	2020-09-05	4.9	279.5	standard
	20201005_135131_66_2277	2020-10-05	5	279.5	standard
	20210316_134737_82_241e	2021-03-16	5.1	279.8	standard
	20210531_134614_85_241e	2021-05-31	5	279.6	standard
	20220505_133805_86_242b	2022-05-05	5	279.3	standard
	20220619_141044_55_24a4	2022-06-19	5	279.5	standard
	20220827_142307_95_2274	2022-08-27	5	279.5	standard
	20230220_132456_32_2445	2023-02-20	5.1	279.3	standard
2	20210603_134145_29_2456	2021-06-03	4	96.3	standard
	20210710_134242_08_2465	2021-07-10	4	96.2	standard
	20210926_142938_21_2274	2021-09-26	4	95.1	standard
	20220602_135219_78_2251	2022-06-02	4	96.4	standard
	20220915_141739_37_227b	2022-09-15	4	96.5	standard
	20221227_140803_96_247d	2022-12-27	4.3	96.3	standard
	20230428_141134_83_2481	2023-04-28	4.4	96.8	standard
3	20200328_134314_64_2263	2020-03-28	0.1	326.7	standard
	20200909_143842_94_227a	2020-09-09	0.1	4.6	standard
	20210420_134520_10_242d	2021-04-20	0	2.8	standard
	20210815_143231_23_2426	2021-08-15	0.1	5	standard
	20211127_133936_00_2455	2021-11-27	0.1	358	test
	20220323_140918_59_2485	2022-03-23	0.1	10.2	standard
	20220823_133629_45_2465	2022-08-23	0.1	0.5	standard
	20221101_140857_70_2490	2022-11-01	0.1	355.7	standard
20230425_141309_40_247b	2023-04-25	0	359.2	standard	
4	20200909_143842_94_227a	2020-09-09	0.1	4.6	standard
	20201114_135258_85_2251	2020-11-14	3.1	280.5	standard
	20210516_134349_86_2235	2021-05-16	5	96.6	standard
	20210710_134242_08_2465	2021-07-10	4	96.2	standard
	20211002_133911_53_2435	2021-10-02	5	96.7	standard
	20220506_140832_67_249d	2022-05-06	2	94.4	standard
	20220610_133641_11_2429	2022-06-10	2.1	94.4	standard
	20220904_135644_53_2276	2022-09-04	4.7	279.4	standard
20230511_133814_07_242d	2023-05-11	1.4	285	standard	

**Table S4.** List of PlanetScope L1B scenes and corresponding metadata used for DEM generation at the Siguas and Del Medio landslide.

<b>Site</b>	<b>Scene ID</b>	<b>Date of Acquisition</b>	<b>View Angle</b>	<b>Satellite Azimuth</b>	<b>Quality</b>
Siguas	20220702_145351_89_240c	2022-07-02	5.1	96.6	standard
	20220706_144107_59_24a3	2022-07-06	5.1	278.7	standard
Del Medio	20220907_140709_64_24a3	2022-09-07	5	96.9	standard
	20220912_141056_91_2486	2022-09-12	5	279.4	standard



## 2 Supplementary figures

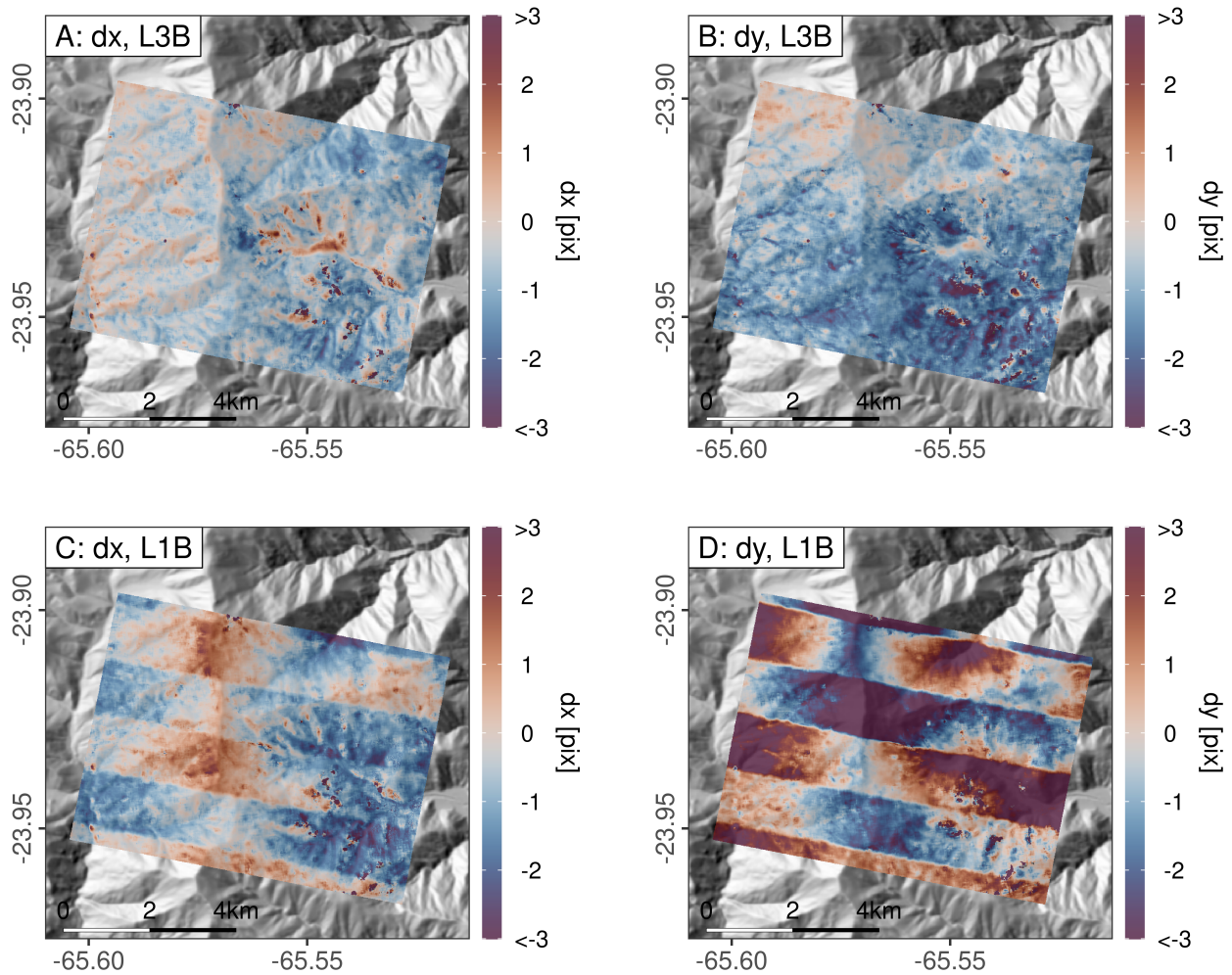


**Figure S1.** Misalignment of sub-frames composing a full PSB.SD scene can cause stripe artifacts in the obtained disparity maps. Particularly older PSB.SD acquisitions (early 2020) are affected. However, Planet seems to have improved the alignment process for newer acquisitions and the L3B data. This Figure shows disparity maps (EW and NS direction) obtained from two PlanetScope scenes acquired on 28.03.2020 and 14.11.2020. In the L3B data, the stripes have disappeared, while the L1B data, which was manually orthorectified using a DEM derived from PlanetScope data, still show severe artifacts.

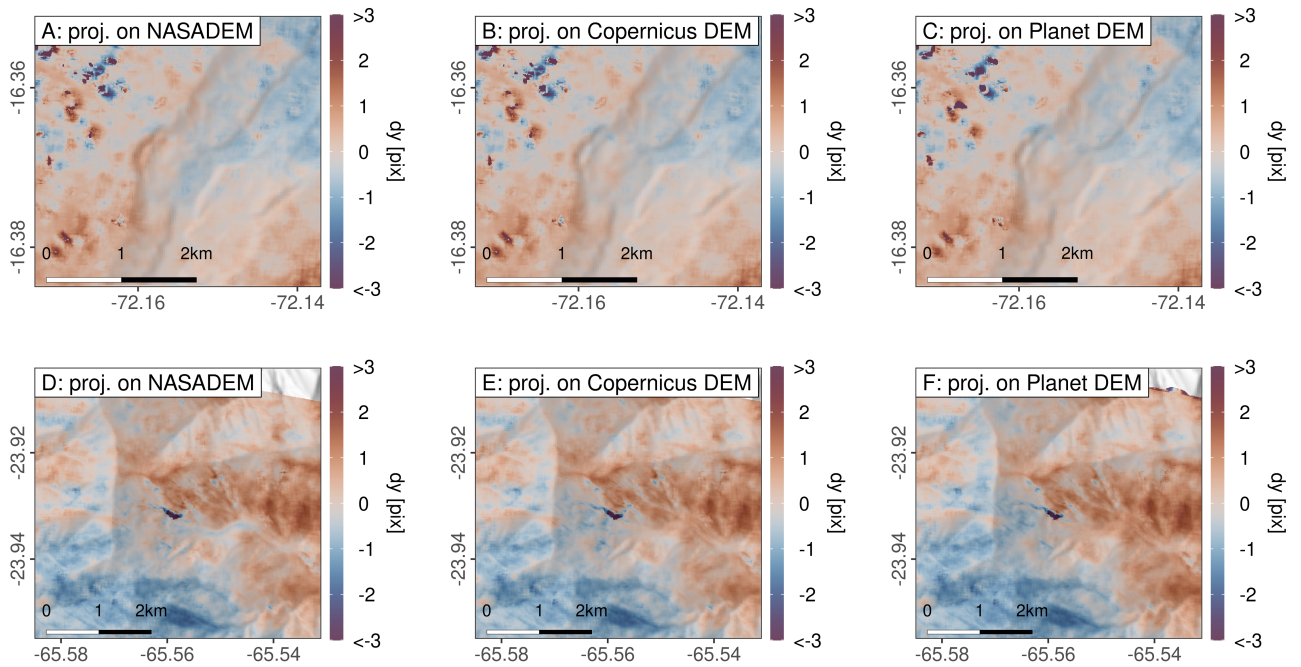


**Figure S2.** Displacement in NS direction estimated across the Siguas (A-C) and Del Medio landslides (D-F) with PlanetScope L1B scenes orthorectified using the NASADEM (A, D), the Copernicus DEM (B, E), and a DEM generated from PlanetScope L1B scenes (C, F). Disparity maps were generated from scene pairs with a minimal temporal baseline (10 days: 07.07.2022 to 17.07.2022) for A-C and 16 days (08.09.2022 to 24.09.2022) for D-F, so the surface can be assumed to be stable. Outdated DEM heights in the reference DEMs produce lateral offset signals in the disparity maps which are, however, less visible in the along-track components.

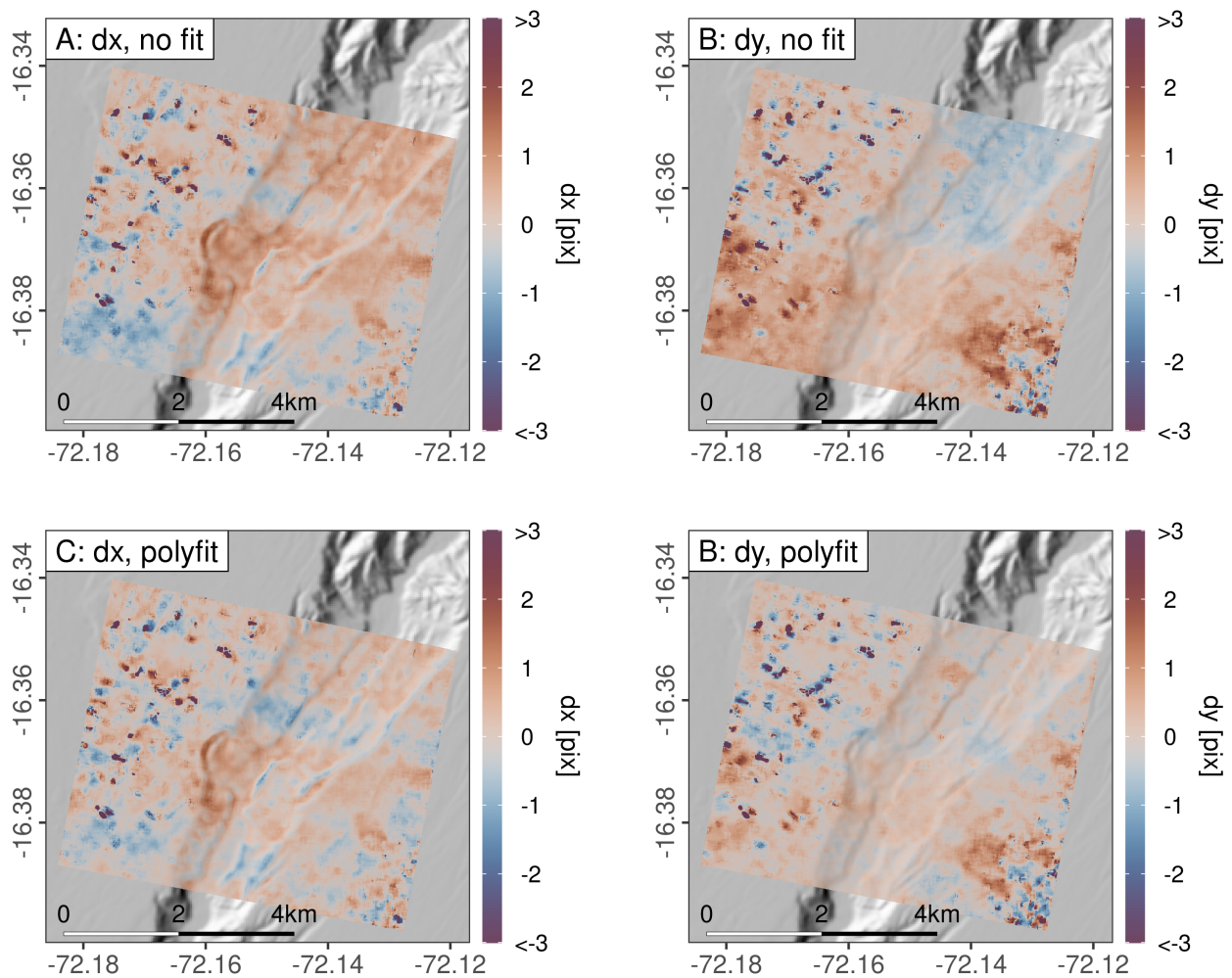


**Figure S3.** Disparity maps estimated across the Siguas landslide based on an L1B scene pair from 07.07.2022 and 17.07.2022 which was projected onto a DEM generated from PlanetScope data. The uncorrected disparity maps (A, B) still show a ramp error which can be efficiently removed by approximating the derived disparity through a polynomial fit. Subtracting this fit results in zero-centered offset maps, which is the expected result for images acquired close in time.



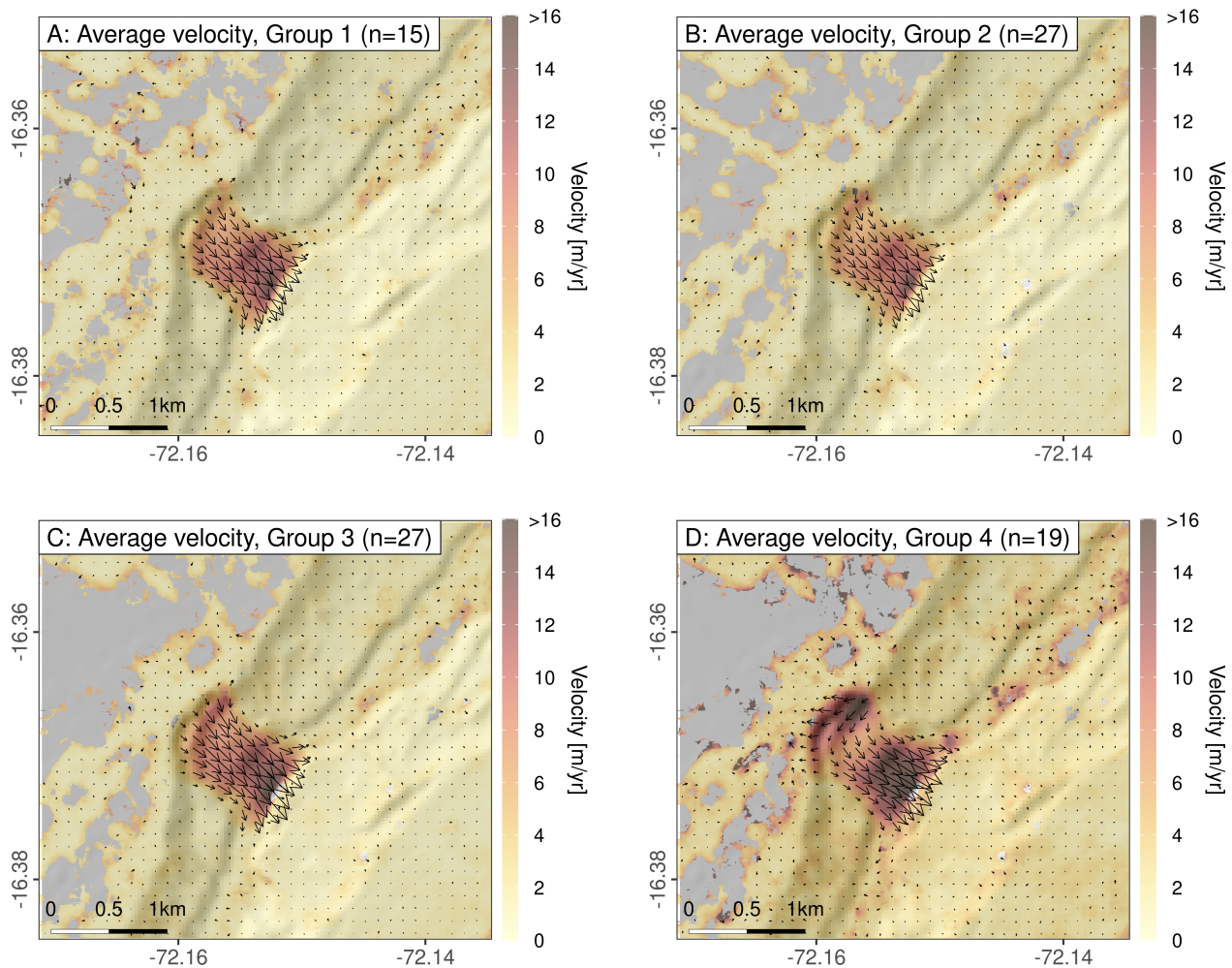


**Figure S4.** Vector plot indicating magnitude and direction of surface displacement estimated across the Sigüas landslide averaged within individual groups sharing a common view angle and satellite azimuth (A-C). Erroneous matches related to changing land cover in the agricultural area towards the northwest of the scene were removed by masking pixels with high standard deviations of velocity. If correlation pairs are not carefully but randomly selected (D), orthorectification errors will propagate to the disparity maps, suggesting elevated velocities and erroneous motion trajectories in areas where elevation changes have occurred. For the average velocity field of group 4, we apply the variance mask from group 3 (C) to mask agricultural areas, as the varying orthorectification error also results high velocity variations across the landslide. All disparity maps used to calculate velocities were optimized using a polynomial fit as described in the main manuscript.

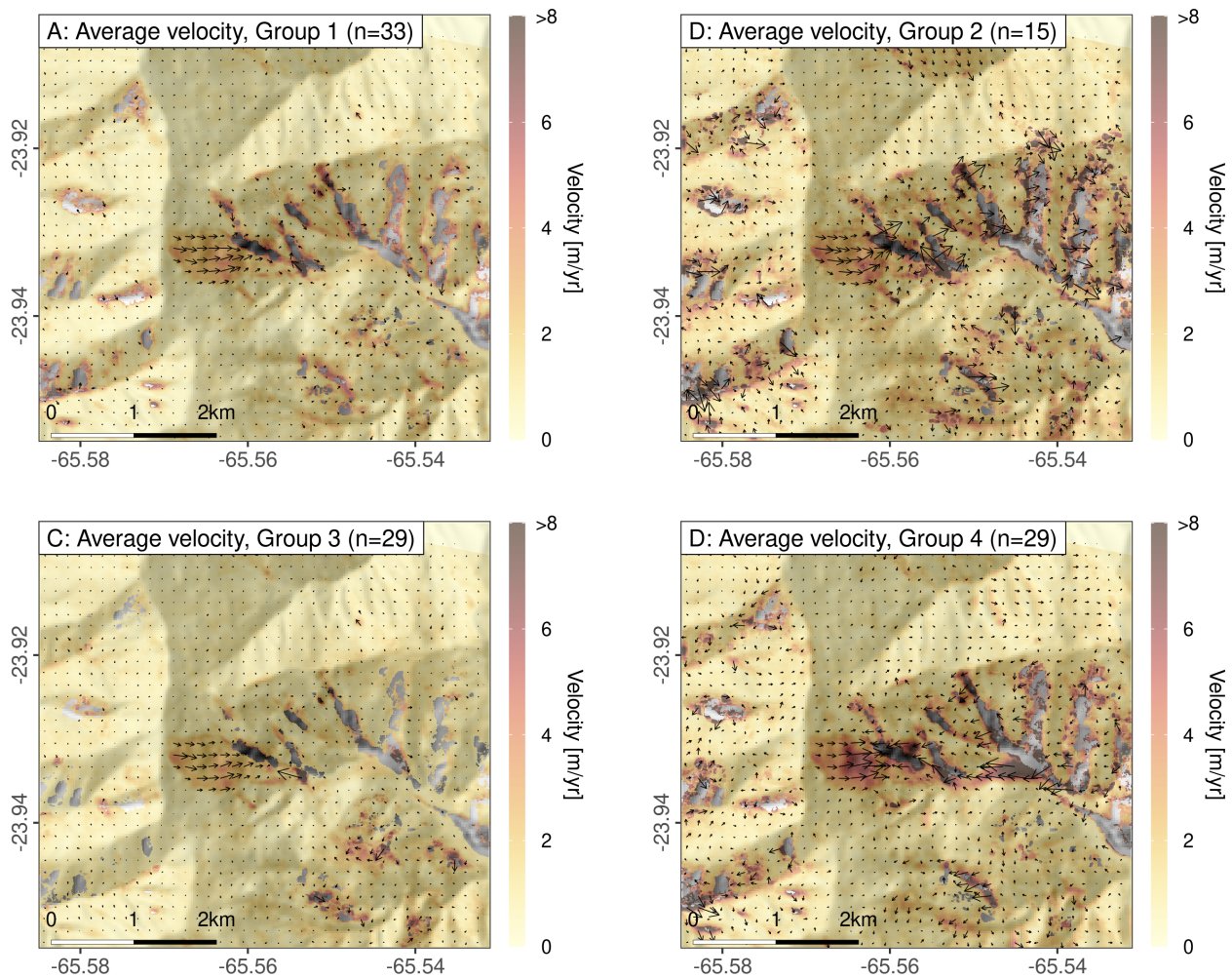


**Figure S5.** Vector plot indicating magnitude and direction of surface displacement estimated across the Del Medio landslide averaged within individual groups sharing a common view angle and satellite azimuth (A-C). Erroneous matches related to variable shading along steep cliffs and deeply incised channels were removed by masking pixels with high standard deviations of velocity. If correlation pairs are not carefully but randomly selected (D), orthorectification errors will propagate to the disparity maps, suggesting elevated velocities and erroneous motion trajectories in areas where elevation changes have occurred. For the average velocity field of group 4, we apply the variance mask from group 3 (C) to mask shadowed areas, as the varying orthorectification error also results high velocity variations across the landslide. All disparity maps used to calculate velocities were optimized using a polynomial fit as described in the main manuscript.

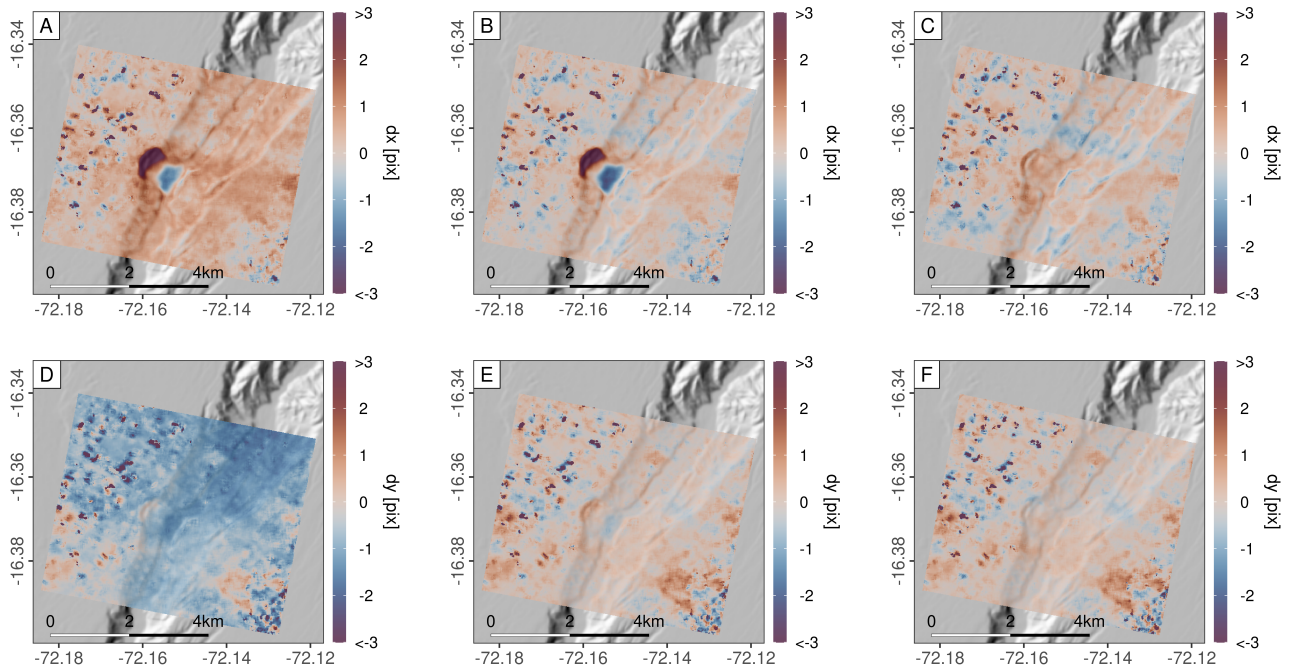


**Figure S6.** Map view of disparity maps in EW ( $dx$ ) and NS ( $dy$ ) directions at the Sigüas landslide derived from two PlanetScope scenes acquired on the 07.07.2022 and 17.07.2022, corresponding to the histograms shown in Figure 14 in the main manuscript. We compare results obtained from Level 3B scenes as downloaded from the Planet Explorer (A, D), after applying a polynomial fit to correct for margin and stereoscopic effects (B, E), and displacement derived from orthorectified L1B scenes using a DEM generated from PlanetScope data, with remaining distortions corrected using a polynomial fit (C, F). Through the correction steps proposed in this study, the coregistration accuracy between two PlanetScope scenes can be lowered to the sub-pixel range over stable terrain, which improves the differentiation of slow landslide motions from noise. Through projecting raw L1B data onto a DEM that more closely aligns with the observed topography, orthorectification errors in the area of the landslide can be significantly reduced.



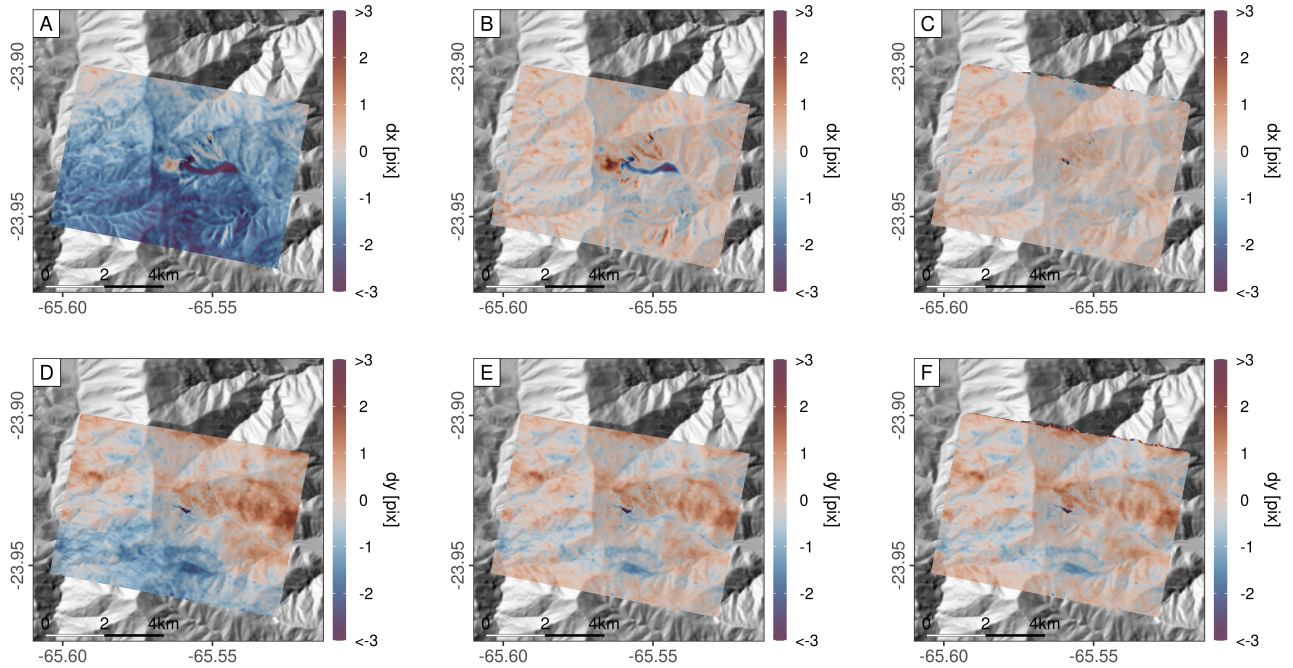


**Figure S7.** Map view of disparity maps in EW ( $dx$ ) and NS ( $dy$ ) directions at the Del Medio landslide derived from two PlanetScope scenes acquired on the 08.09.2022 and 24.09.2022, corresponding to the histograms shown in Figure 14 in the main manuscript. We compare results obtained from Level 3B scenes as downloaded from the Planet Explorer (A, D), after applying a polynomial fit to correct for margin and stereoscopic effects (B, E), and displacement derived from orthorectified LIB scenes using a DEM generated from PlanetScope data, with remaining distortions corrected using a polynomial fit (C, F). Through the correction steps proposed in this study, the coregistration accuracy between two PlanetScope scenes can be lowered to the sub-pixel range over stable terrain, which improves the differentiation of slow landslide motions from noise. Through projecting raw LIB data onto a DEM that more closely aligns with the observed topography, orthorectification errors in the area of the landslide can be significantly reduced.

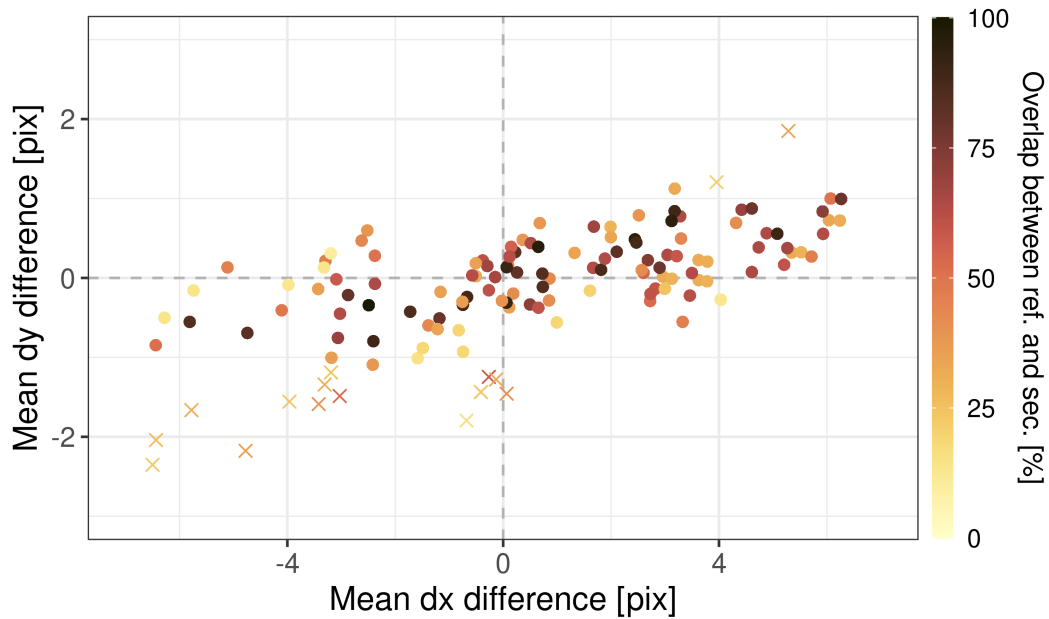


**Figure S8.** Difference of mean displacement in EW (dx) and NS (dy) directions between source and deposition area of the Sigvas landslide derived from 136 correlation pairs of L3B scenes between July 7 and August 23, 2022. Colors represent overlap between reference and secondary scene in percent. We find no relationship between those two parameters, indicating that the local incidence angle within a scene is negligible for predicting the orthorectification error.

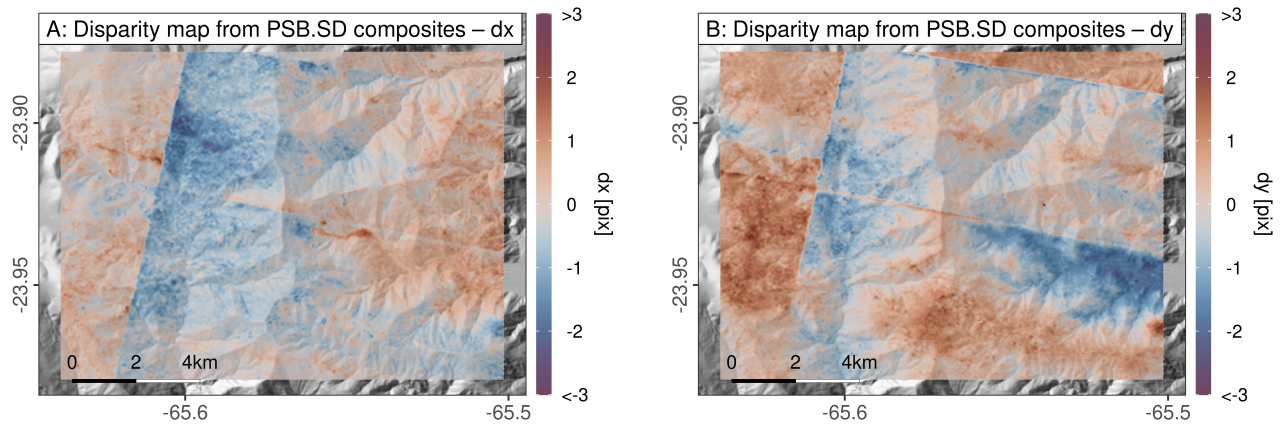


**Figure S9.** Disparity maps in EW and NS direction obtained from two PlanetScope data composites downloaded from the Planet Explorer. The estimated offset clearly reflects the margins of the composited scenes with sudden jumps of approx. 2 pixels. Given these severe artifacts, we recommend to manually improve the stitching process if slow motions across larger study areas are targeted.